OPEN

Oncogene (2013) 32, 5347–5358

www.nature.com/onc

ORIGINAL ARTICLE

The costimulatory molecule B7-H4 promote tumor progression and cell proliferation through translocating into nucleus

L Zhang[1,2,6], H Wu[3,6], D Lu[1], G Li[1,4], C Sun[5], H Song[2], J Li[2], T Zhai[2], Lv Huang[2], C Hou[5], W Wang[2], B Zhou[3], S Chen[2], B Lu[4] and X Zhang[1]

B7-H4, a member of B7 family, is a transmembrane protein and inhibits T-cells immunity. However, in a variety of tumor cells, B7-H4 was detected predominantly in intracellular compartments with unknown mechanism and functions. In this study, we analyzed B7-H4 expression and subcellular distribution by immunohistochemistry in renal cell carcinoma (RCC) tissues. B7-H4 protein was detected on the membrane, in the cytosol and/or in the nucleus in tumor tissues. The membrane and nuclear expression of B7-H4 was significantly correlated with the tumor stages of RCC. Moreover, the membrane localization of B7-H4 was inversely correlated with the intensity of tumor infiltrates lymphocyte (TILs), whereas no association was observed between nuclear expression of B7-H4 and the density of TILs status. We further identified that B7-H4 is a cytoplasmic-nuclear shuttling protein containing a functional nuclear localization sequence (NLS) motif. A point mutation of B7-H4 NLS motif blocked the leptomycin B -induced nuclear accumulation of B7-H4. HEK293 cells stably expressing B7-H4 NLS mutant exhibited more potent inhibition in T-cell proliferation and cytokine production through increasing its surface expression compared with wild-type B7-H4 transfected cells owing to their increased surface expression. Most importantly, overexpression of wild-type B7-H4 in HEK293 cells enhanced tumor cell proliferation *in vitro* and tumorigenicity *in vivo*, promoted G1/S phase transition. The regulation of cell cycle by wild-type B7-H4 was partialy due to upregulation of Cyclin D 1 and Cyclin E. A mutation of B7-H4 NLS motif abolished the B7-H4-mediated cell proliferation and cell cycle regulation. Furthermore, B7-H4 wild-type confers chemoresistance activity to RCC cell lines including Caki-1 and ACHN. Our study provides a new insight into the functional implication of B7-H4 in its subcellular localization.

Oncogene (2013) **32,** 5347–5358; doi:10.1038/onc.2012.600; published online 14 January 2013

Keywords: B7-H4; nuclear localization sequence (NLS); tumor infiltrated lymphocyte (TIL); renal cell carcinoma (RCC); cell cycle; cell proliferation

INTRODUCTION

The costimulatory B7 family members are cell-surface protein ligands, binding to receptors on lymphocytes to regulate immune responses. They not only provide positive signals to stimulate T-cell activation, but also deliver negative signals to inhibit T-cell responses. The growing B7 family consists of seven members, B7.1 (CD80), B7.2 (CD86), B7-DC (CD273, PD-L2), B7-H1 (CD274, PD-L1), B7-H2 (ICOS-L), B7-H3 (CD276) and B7-H4 (B7x, B7S1). Accumulating evidence has demonstrated that inhibitory B7 molecules are frequently upregulated in different tumors, which may contribute to tumor immune evasion. In the tumor microenvironment, enhanced expression of inhibitory B7 molecules may inhibit T-cell activation, ultimately protecting tumor cells from effective T-cell destruction.[1]

B7-H4, a member of the B7 family that was independently discovered by three groups in 2003, has been identified as a negative regulatory molecule on the cell membrane, which inhibits the proliferation and cytokine production of $CD4^+$ and $CD8^+$ T cells.[2–4] The overexpression of B7-H4 has been found in various types of human tumors, such as breast cancer,[5] renal cell carcinoma (RCC),[6] ovarian cancer,[7–9] esophageal squamous cell carcinoma,[10] gastric cancer,[11,12] pancreatic cancer[13] and melanoma[14] etc. Furthermore, the expression level of B7-H4 is positively correlated with disease progression.[1]

B7-H4 is a well-defined transmembrane protein, which contains signal peptide and hydrophobic transmembrane domain.[2–4] However, some tumor cells were shown to express B7-H4 protein in intracellular compartment. Kryczed *et al.*[7] reported that B7-H4 was predominantly expressed in the intracellular compartments of ovarian tumor cells. Unlike tumor-associated macrophages with membrane-bound B7-H4, ovarian tumor cells expressing intracellular B7-H4 do not suppress T-cell immunity, suggesting a distinct function of intracellular B7-H4 from membrane-bound B7-H4. In addition, intracellular expression of B7-H4 was found in all the melanoma cell lines tested whereas B7-H4 surface expression was not detectable.[14] So far, the mechanisms and functional implications of B7-H4 subcellular localization remain unclear.

RCC is an immunogenic tumor with the high level of tumor T-cell infiltration. Patients with advanced disease have a poor prognosis, with a 5 year survival rate of less than 10%. Previous studies showed that inhibitory B7 family members B7-H1 and B7-H4 have a high frequency of overexpression in RCC and associated with increased disease progression and decreased cancer-specific

[1]Jiangsu Stem Cell Key Laboratory, Institute of Medical Biotechnology, Medical College of Soochow University, Suzhou, China; [2]Department of Pharmacy, College of Pharmaceutical Science, Soochow University, Suzhou, China; [3]Jiangsu Institute of Clinical Immunology, The first affiliated hospital of Soochow University, Suzhou, China; [4]Department of Immunology, University of Pittsburgh, Pittsburgh, PA, USA and [5]The Department of Urology, The second affiliated hospital of Soochow University, Suzhou, China. Correspondence: Professor X Zhang, Jiangsu Stem Cell Research Laboratory, Institute of Medical Biotechnology, Medical College of Soochow University, Renmin Road, 178, Suzhou 215006, China.
E-mail: xueguangzh@yahoo.com.cn
[6]These authors contributed equally to this paper.
Received 12 April 2012; revised 6 November 2012; accepted 8 November 2012; published online 14 January 2013

survival. In this study, we examined the subcellular distribution of B7-H4 in 82 clinical RCC tissues by immunohistochemical analysis. Our results showed that the B7-H4 protein was expressed on the plasma membrane, in the cytosol and/or in the nucleus of tumor cells in RCC tissues. The membrane and nuclear expressions of B7-H4 were correlated with tumor stage. We further showed that the B7-H4 molecule contains a functional nuclear localization sequence (NLS), which is responsible for nuclear distribution of B7-H4. A point mutation of B7-H4 NLS motif suppressed the LMB-induced nuclear accumulation of B7-H4. Very importantly, B7-H4 overexpression in HEK293 cells stimulated proliferation *in vitro* and promoted G1/S phase transition. The mutation of B7-H4 NLS abrogated B7-H4-mediated proliferation and cell cycle progression. These results indicated that nuclear localization of B7-H4 might be crucial for B7-H4-mediated proliferation and cell cycle progression.

RESULTS

The expression pattern of B7-H4 in RCC

A total of 82 specimens were collected from RCC patients who were treated by radical nephrectomy. Immunohistochemical analysis was used to examine B7-H4 expression. The different expression patterns of B7-H4 were observed. Positive membranous, cytoplasmic and nuclear staining were detected in 36 cases (43.9%), 42 cases (51.2%) and 33 cases (40.2%), respectively (Table 1 and Figure 1). We further showed that the membranous and nuclear expression of B7-H4 were significantly associated with tumor classification, 2002 Tumor, Node, Metastasis (TNM) stage grouping and nuclear grade (Table 1), suggesting that the membrane and nuclear localization of B7-H4 might be correlated with clinical outcome in RCC. The immunostaining analysis of CD4+ and CD8+ T-cells indicated the membrane B7-H4 was inversely correlated with the density of tumor infiltrates lymphocyte (TILs). However, no significant association was seen between the nuclear B7-H4 and the density of TILs (Table 1). We also evaluated the average Allred score of membrane B7-H4 and nuclear B7-H4, and found that average membrane B7-H4 expression level or nuclear B7-H4 expression level was significantly increased in higher-grade tumors compared with that in lower-grade tumors (Supplementary Figures 1A and B). Average Allred score of membrane B7-H4 was significantly increased in M1 stage compared with that in M0 stage ($P = 0.002$, Supplementary Figure 1C), while nuclear B7-H4 expression did not significantly differ in M1 and M0 ($P = 0.114$, Supplementary Figure 1D). In addition, we observed a significant increase in the average density of CD4+ or CD8+ T-cells infiltration in membrane B7-H4-negative specimen compared with that in membrane B7-H4-positive specimen ($P = 0.009$ for CD4+ T cells and $P = 0.015$ for CD8+ T cells, Supplementary Figures 1E and F). However, the density of TILS did not change significantly in nuclear B7-H4-negative or positive specimen ($P = 0.354$ for CD4+ T cells and $P = 0.371$ for CD8+ T cells, Supplementary Figures 1G and H).

Human B7-H4 contains a putative NLS motif and is a cytoplasmic-nuclear shuttling protein

To identify a potential NLS motif in the B7-H4 protein sequence, the coding region of human B7-H4 was analyzed using the predictNLS program (http://cubic.bioc.columbia.edu/predictNLS). The sequence KRRSH (246–250) was identified as a potential NLS motif (Figure 2a). Unlike human B7-H4, no specific NLS was predicted in murine B7-H4 by this program (Figure 2a). The homology of KRRSH in murine B7-H4 was KRRSQ. To determine the subcellular localization of B7-H4 in transfected living cells, we generated an expression construct encoding human B7-H4 fused to the N-terminus of green fluorescent protein (GFP). The construct was stably transfected into HEK293 cells (Figure 2d). Fluorescence microscopy showed that B7-H4-GFP was mainly localized in the cytoplasm (Figure 2e). The cytoplasmic localization might be the result of rapid nuclear export relative to nuclear import. To test this possibility, we treated cells expressing B7-H4-GFP with leptomycin B (LMB), a specific inhibitor of nuclear export receptor CRM1. LMB treatment resulted in a significant increase in B7-H4-GFP nuclear localization (Figure 2e). This result suggests that B7-H4 could shuttle between the nucleus and cytoplasm. To test whether the putative NLS motif is sufficient to direct B7-H4 nuclear import, a point mutation in the NLS was made by site-mutagenesis to change His-250 to Gln (Figures 2b and c). This mutation suppressed the LMB-induced nuclear localization of B7-H4-GFP (Figure 2e). This demonstrates the presence of a functional NLS motif in B7-H4 protein sequence. Consistent with this, line intensity scan using Leica LAS AF (Leica Application Suite Advanced Fluorescence, Leica Microsystems, Mannheim, Germany) software showed that LMB treatment enhanced cy5 fluorescence intensity (blue) in the nucleus of HEK293 cells stably expressing B7-H4, but had no effect on cy5 fluorescence intensity in B7-H4 H250Q transfected cells (Figure 2f).

Subcellular localization of B7-H4 in tumor cells

As the GFP tag may affect subcellular localization of some tagged proteins, we next investigate the subcellular distribution of the endogenous B7-H4 in tumor cells. Three different B7-H4 specific antibodies were used to detect B7-H4 expression. These antibodies include a monoclonal antibody (mAb) clone 3C8 directed against extracellular epitope of B7-H4, a polyclonal antibody G-18 directed against the epitope near the N-terminus and a polyclonal antibody H-108 against the epitope corresponding to the C-terminus. The SK-BR-3 cells were selected to examine B7-H4 localization because this cell line has a well-documented high expression of B7-H4. As shown in Figure 3a, B7-H4 was predominantly expressed in the cytoplasm. Treatment with LMB significantly enhanced nuclear staining of B7-H4. As a control, the endoplasmic reticulum marker, calnexin did not translocate into the nucleus in the presence of LMB. Three independent B7-H4 antibodies give the same staining pattern. The B7-H4 cDNA was amplified from SK-BR-3 cells and sequenced. No mutation was found in the whole coding region of the *B7-H4* gene. Taken together, we reasoned that full-length wild-type B7-H4 protein could shuttle between the nucleus and the cytoplasm in SK-BR-3 cells.

We further assessed the subcellular localization of B7-H4 protein using biochemical fractionation. SK-BR-3 cells were treated with LMB or vehicle alone. The cells were then fractionated into cytoplasmic and nuclear components. The fractions were analyzed by immunoblot. In the absence of LMB, the B7-H4 protein was undetectable in nuclear fraction. Treatment with LMB led to a dramatic increase in nuclear level of B7-H4 (Figure 3b).

In addition, we examined the effect of LMB on subcellular localization of B7-H4 in MDA-MB-453, MCF-7, U937and THP-1 cells using confocal immunofluorescence microscopy, LMB treatment caused nuclear accumulation of B7-H4 protein in all cell lines tested (Figure 3c).

The effects of wild-type B7-H4 and NLS mutated B7-H4 on negative regulation of T-cell activation

As B7-H4 has been shown to serve as a negative regulator of T-cell immunity, we tested the effect of B7-H4 NLS motif on its negative regulatory function. Purified human T cells were cocultured with stably transfected HEK293 cells expressing GFP or B7-H4-GFP or B7-H4-H250Q-GFP. As expected, wild-type B7-H4 transfectants inhibited T-cell proliferation. By note, the NLS mutant transfectants exhibited a stronger inhibitory effect on T-cell proliferation than wild-type B7-H4 transfected cells (Figure 4a). Moreover, cocultured with NLS mutant transfectants resulted in a significantly lower levels of IL(interleukin)-2, IL-10 and

Table 1. Correlation of B7-H4 three expression patterns in RCC tissues and clinicopathological parameters.

Variables	*B7-H4 membrane expression, n (%)*			*B7-H4 cytosol expression, n (%)*			*B7-H4 nuclear expression, n (%)*		
	Positive[a]	*Negative*[a]	P-*value*	*Positive*[a]	*Negative*[a]	P-*value*	*Positive*[a]	*Negative*[a]	P-*value*
Age (yr)									
<60	22 (61.1)	30 (65.2)	0.702[b]	24 (57.1)	28 (70.0)	0.227[b]	19 (57.6)	33 (67.3)	0.368[b]
$\geqslant 60$	14 (38.8)	16 (34.8)		18 (42.9)	12 (30.0)		14 (42.4)	16 (32.7)	
Gender									
Male	23 (63.9)	24 (52.2)	0.287[b]	26 (61.9)	21(52.5)	0.389[b]	19 (57.6)	28 (57.1)	0.969[b]
Female	13 (36.1)	22 (47.8)		16 (38.1)	19 (47.5)		14 (42.4)	21 (42.9)	
Symptoms at presentation									
Absent	29 (80.6)	34 (73.9)	0.479[b]	31 (73.8)	32 (80.0)	0.507[b]	24 (72.7)	39 (79.6)	0.470[b]
Present	7 (19.4)	12 (26.1)		11 (26.2)	8 (20.0)		9 (27.3)	10 (20.4)	
Primary tumor size (cm)									
<4 cm	18 (50.0)	18 (39.1)	0.417[b]	16 (38.1)	20 (50.0)	0.549[b]	12 (36.4)	24 (49.0)	0.487[c]
4–7 cm	12 (33.3)	22 (47.8)		19 (45.2)	15 (37.5)		15 (45.5)	19 (38.8)	
>7 cm	6 (16.7)	6 (13.0)		7 (16.7)	5 (12.5)		6 (18.2)	6 (12.2)	
2002 primary tumor classification									
pT1	11 (30.6)	31 (67.4)	0.003[c]	23 (54.8)	19 (47.5)	0.730[c]	9 (27.3)	33 (67.3)	0.001[c]
pT2	17 (47.2)	12 (26.1)		15 (35.7)	14 (35.0)		16 (48.5)	13 (26.5)	
pT3	5 (13.9)	3 (6.5)		3 (7.1)	5 (12.5)		5 (15.2)	3 (6.1)	
pT4	3 (8.3)	0		1 (2.4)	2 (5.0)		3 (9.1)	0 (0.0)	
Regional lymph node involvement									
pNx/pN0	32 (88.9)	45 (97.8)	0.163[c]	38 (90.5)	39 (97.5)		30 (90.9)	47 (95.9)	0.387[c]
PN1/pN2	4 (11.1)	1 (2.2)		4 (9.5)	1 (2.5)		3 (9.1)	2 (4.1)	
Distant metastases at nephrectomy									
pM0	27 (75.0)	43 (93.5)	0.019[b]	33 (78.6)	37 (92.5)	0.074[b]	27 (81.8)	43 (87.8)	0.531[c]
pM1	9 (25.0)	3 (6.5)		9 (21.4)	3 (7.5)		6 (18.2)	6 (12.2)	
2002 TNM stage groupings									
I	9 (25.0)	31 (67.4)	0.001[c]	21 (50.0)	19 (47.5)	0.288[c]	9 (27.3)	31 (63.3)	0.012[c]
II	11 (30.6)	9 (19.6)		8 (19.0)	12 (30.0)		11 (33.3)	9 (18.4)	
III	5 (13.9)	3 (6.5)		3 (7.1)	5 (12.5)		5 (15.2)	3 (6.1)	
IV	11 (30.6)	3 (6.5)		10 (23.8)	4 (10.0)		8 (24.2)	6 (12.2)	
Nuclear grade									
1	3 (8.3)	8 (17.4)	0.012[c]	3 (7.1)	8 (20.0)	0.346[b]	2 (6.1)	9 (18.4)	0.030[c]
2	7 (19.4)	21 (45.7)		15 (35.7)	13 (32.5)		8 (24.2)	20 (40.8)	
3	18 (50.0)	14 (30.4)		17 (40.5)	15 (37.5)		15 (45.5)	17 (34.7)	
4	8 (22.2)	3 (6.5)		7 (16.7)	4 (10.0)		8 (24.2)	3 (6.1)	
Densitiy of CD4+ cells (cells per high-power field)									
Low	26 (72.2)	23 (50.0)	0.042[b]	24 (57.1)	25 (62.5)	0.621[b]	21 (63.6)	28 (57.1)	0.557[b]
High	10 (27.8)	23 (50.0)		18 (42.9)	15 (37.5)		12 (36.4)	21 (42.9)	
Densitiy of CD8+ cells (cells per high-power field)									
Low	26 (72.2)	19 (41.3)	0.005[b]	22 (52.4)	23 (57.5)	0.641[b]	18 (54.5)	27 (55.1)	0.960[b]
High	10 (27.8)	27 (58.7)		20 (47.6)	17 (42.5)		15 (45.5)	22 (44.9)	

Abbreviations: RCC, renal cell carcinoma; TNM, tumor node metastasis. [a]Cutpoint for positive: Allred score >3; cut point for negative: Allred score $\leqslant 3$. [b]Pearson chi-square, Asump. Sig., two sided. [c]Fisher exact test, Exact. Sig., two sided.

interferon - γ compared with wild-type transfectants (Figures 4b-d). These results imply that stable transfected HEK293 cells could express functional wild-type and mutated B7-H4 protein on cell surface.

Previous studies demonstrated that B7-H4 could exist in a soluble form.[8] To determine whether B7-H4 stably transfected HEK293 cells produced soluble B7-H4 protein, the supernatants were collected from either wild-type or NLS mutant transfectants, and analyzed by immunoblotting using B7-H4 specific antibody. The soluble B7-H4 was detected in the supernatants from stable transfected HEK 293 cells expressing either wild-type or NLS mutated B7-H4. Surprisingly, NLS mutant stably transfected cells produced markedly more soluble B7-H4 than did wild-type transfectants. Treatment with minnesota multiphasic personality inventory (MMPI) dramatically reduced the level of soluble B7-H4 (Figure 4e). These results indicated that NLS mutation of B7-H4 increased the cell surface expression of B7-H4, which might be cleaved and released as a soluble form by MMP.

To confirm the results from coculture experiment, magnetic selection CD4+ and CD8+ T cells were treated with the supernatants from either wild-type or NLS mutant transfectants. Treatment with the supernatants from mutant transfectants exhibited more potent inhibition in T-cell proliferation and IL-2 production relative to the supernatant from wild-type

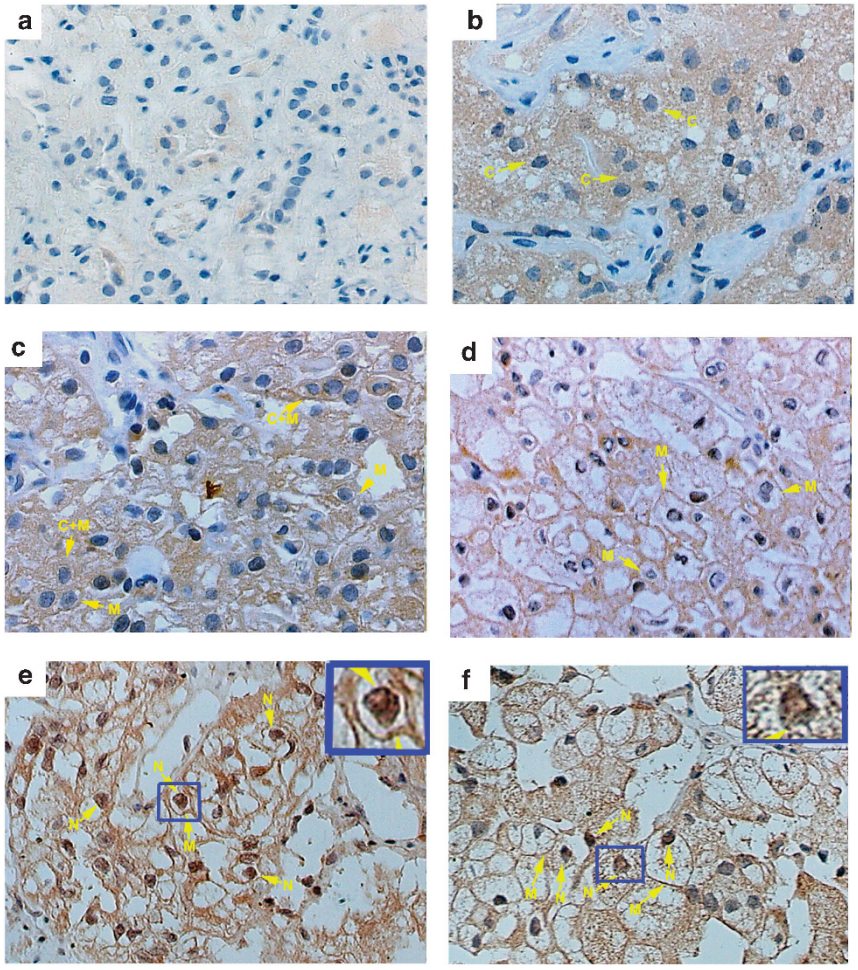

Figure 1. Representative immunohistochemical staining of B7-H4 in RCC tissues using anti-B7-H4 mAb 3C8. (magnification × 400) (**a**) Negative control. (**b**) B7-H4 was predominantly expressed in the cytosol. (**c**) B7-H4 was predominantly expressed on the membrane and in the cytosol. (**d**) B7-H4 was predominantly localized on the membrane. (**e**) and (**f**) B7-H4 was predominantly localized on the membrane and in the nucleus.

transfectants (Figures 4f and g). Furthermore, the T-cell inhibition of supernatants from mutant transfectants was efficiently blocked by anti-B7-H4 mAb (3C8) (Figures 4f and g), suggesting B7-H4-dependent T-cell inhibition.

Nuclear localization of B7-H4 is crucial for B7-H4-induced cell proliferation and G1/S phase transition

Somewhat surprisingly, we observed an increased rate of proliferation of wild-type B7-H4 stably transfected cells (Figure 5a), while proliferation rates of B7-H4 H250Q transfected cells were comparable with cells stably transfected with the empty vector. This suggests that the NLS mutation of B7-H4 could abrogate its ability to regulate cell proliferation. To explore the mechanism by which wild-type B7-H4 regulates cell proliferation, the cell cycle distribution of HEK293 cells stably transfected with pIRES2-EGFP vector or with pIRES2-EGFP-B7-H4 or with pIRES2-EGFP-B7-H4-H250Q were determined by flow cytometry. The percentage of B7-H4 WT/293 cells in G1 phase was obviously reduced in comparison with mock/293 and B7-H4 H250Q MT/293 cells (40.43 ± 3.88vs 51.06 ± 1.25% and 48.42 ± 2.45, $P = 0.011$ and $P = 0.039$, respectively) (Figure 5b). Moreover, we found that B7-H4 wild-type regulated the cell cycle by upregulating Cyclin D1 and Cyclin E in HEK293 cells, whereas B7-H4 NLS mutation had no effect on the expression of these two molecules (Figure 5c). We implanted HEK 293 cells expressing empty vector, B7-H4 WT, or B7-H4 H250Q MT, in severe combined immunodeficiency mice mixed with matrigel by subcutaneous injection at a dose of 2×10^7 cells/mouse. In the group that mice were implanted with two different cells on contralateral sides, it was observed that B7-H4 WT/293 cells formed larger tumors than Mock/293 cells and B7-H4 H250Q MT/293 cells, while in the group that mice injected with Mock/293 and B7-H4 H250Q MT/293 cells on two sides, respectively, there was no significant difference in tumor size (Figure 5d). Furthermore 24 severe combined immunodeficiency mice were divided into three groups and in each group, eight mice were injected with Mock/293, B7-H4 WT/293 or B7-H4 H250Q MT/293 cells, respectively. It was observed that tumor growth was significantly enhanced when measured on 8th week in the group injected with B7-H4 WT/293 cells ($175.2 \pm 118.4\,mm^3$) compared with the group injected with Mock/293 cells ($70.8 \pm 42.2\,mm^3$) or the group injected with B7-H4 H250Q MT/293 cells ($64.0 \pm 62.9\,mm^3$) (Figure 5d). Difference of tumor weight between the three groups was also observed (96.5 ± 46.0 vs 43.8 ± 28.6 mg in B7-H4 WT/293 and Mock/293, respectively, $P = 0.016$; 96.5 ± 46.0 vs 35.9 ± 28.7 mg in B7-H4 WT/293 and B7-H4 H250Q MT/293, respectively, $P = 0.007$; Figure 5e). Immunohistochemical staining showed that B7-H4 was highly expressed in xenograft tumor tissues derived from B7-H4 WT/293 and B7-H4 H250Q MT/293 cells, but rarely expressed in xenograft tissues from Mock/293 cells (Supplementary Figures 2A, B and C). Furthermore, we observed that B7-H4 was expressed not only on the membrane or

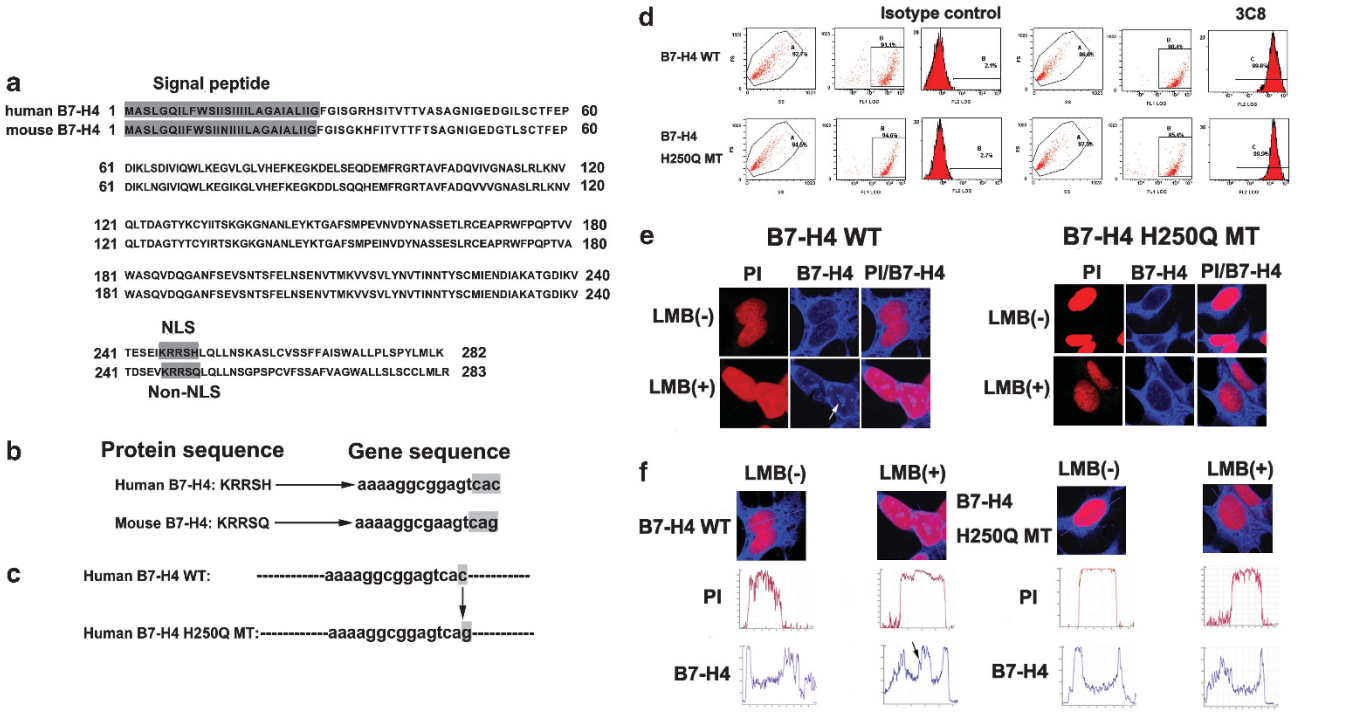

Figure 2. The NLS motif in B7-H4 protein. (**a**) Comparison of human and mouse B7-H4 sequence. Signal peptide and NLS motif were shaded in gray. (**b**) Contrast to human B7-H4, mouse homolog lacks a consensus NLS motif. The crucial nucleotides for NLS were shaded in gray. (**c**) A point mutation of human B7-H4 NLS motif. At nucleotide position 750, C was changed to G, resulting in a change from His to Gln at amino acid position 250. (**d**) Flow cytometric analysis of either B7-H4 WT/293 or B7-H4 H250Q MT/293 transfectants showed that the stable transfected cell lines were successfully constructed. (**e**) The B7-H4 transfectants and B7-H4 H250Q transfectants were examined by confocal immunofluorescent microscopy in the absence or presence of LMB. The anti-B7-H4 mAb 3C8 was used. White arrows indicated the nuclear localization of B7-H4 (PI (red, DNA) and cy5 (blue, B7-H4)). (**f**) The merged images were subjected to line intensity scan using Leica LAS AF software to assess the localization of B7-H4. Intensity profiles corresponding to the lines were determined using Leica LAS AF software. Y- and X-axes represent the level of fluorescence and scanning position, respectively. The black arrows indicated the presence of blue fluorescence in red fluorescence, which suggest the existence of B7-H4 in nucleus.

cytoplasm, but also in nucleus in the xenograft tissues from B7-H4 WT/293 cells, whereas B7-H4 was not expressed in nucleus in xenograft tissues from B7-H4 H250Q MT/293 cells (Supplementary Figure 2B, blue arrows indicated). Thus, our results indicated that nuclear localization of B7-H4 may have a crucial role in B7-H4-mediated cell proliferation and cell cycle progression.

The effect of nuclear B7-H4 in RCC cell lines

As we have demonstrated that the nuclear localization pattern of B7-H4 in RCC tissue and found that nuclear B7-H4 was associated with tumor stage, we further investigated the function of B7-H4 in RCC cells. We detected the RCC cell lines 786-O, Caki-1 and ACHN, and found that these RCC cell lines did not express membrane or intracellular B7-H4 (Figure 6a). To study the function significance of B7-H4, Caki-1 and ACHN, cells were transfected with expression plasmids pIRES2-EGFP-B7-H4 and pIRES2-EGFP-B7-H4-H250Q and vector alone. GFP + cells were selected using flow cytometry at 24 h after transfection. The mAb 3C8 staining showed that these GFP + cells also positively expressed B7-H4 (Figure 6b). These GFP + cells selected by flow cytometry were seeded into 96-well plates and cultured in 10% fetal bovine serum/Dulbecco's modified eagle Media (FBS/DMEM) medium. Cell proliferations were quantified by CCK8 at 24, 48 and 72 h. As shown in figure 6c, B7-H4 WT/Caki-1 cells exhibited a significant proliferation index at 72 h compared with Mock/Caki-1 and B7-h4 H250Q MT/Caki-1. When cells were treated with doxorubicin or docetaxel, B7-H4 WT conferred antiapototic ability to Caki-1 (Figure 6d) and ACHN cells, (Figure 6e) while B7-H4 H250Q MT could not. These results showed that B7-H4 WT could act as an antiapoptosis molecule in RCC cell lines, which might contribute to disease progression.

DISCUSSION

Previous studies have demonstrated that the B7-H4 molecule is highly expressed in many different types of human cancers and mostly associated with poor clinical outcomes. In contrast, the B7-H4 protein is not detected in majority of normal human tissues.[1] B7-H4 is also expressed by a variety of normal lymphoid cells, and functions as a negative mediator of T-cell activity. In contrast to its surface expression by normal lymphoid cells, B7-H4 protein exhibits different subcellular distributions in cancer cells. Some melanoma cells exclusively expressed intracellular rather than cell surface B7-H4 protein.[14] In the lung and ovarian cancer cells, B7-H4 has been found to express either cytoplasm or plasma membrane.[1,9] Miyatake *et al.*[15] reported that the B7-H4 protein was typically located to the apical cytoplasmic membrane in normal or hyperplasic endomentrium, but showed intense circumferential membranous and cytoplasmic expression in most endometrial and ovarian endometrioid carcinomas. Here, we revealed that the B7-H4 protein was expressed on the plasma membrane, in the cytosol and/or in the nucleus in RCC tissues. The membranous and nuclear localizations of B7-H4 were significantly associated with disease progression. Membrane B7-H4 was inversely correlated with the density of TILs, whereas nuclear B7-H4 demonstrated no correlation with TILs. The results extend previous studies on subcellular distribution of B7-H4 in tumor tissues with clinical significance. Membrane B7-H4 might promote

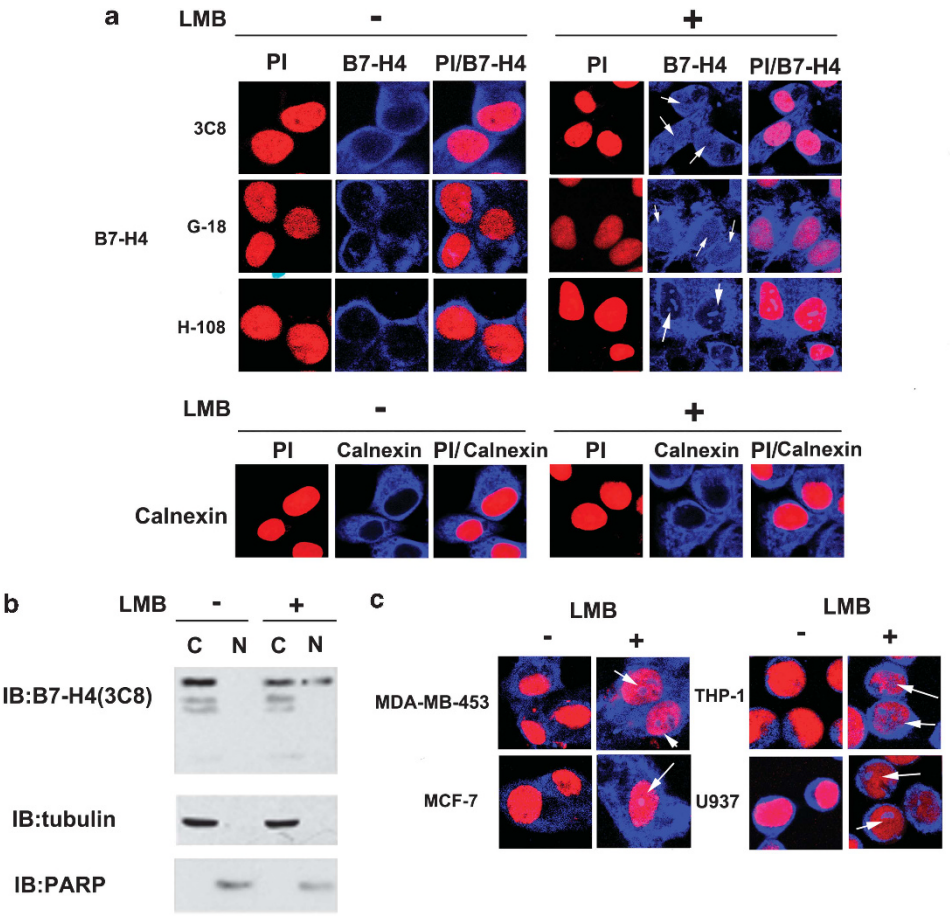

Figure 3. Subcellular localization of B7-H4 in different cancer cell lines. (**a**) Confocal immunofluorescent microscopy demonstrated a nuclear translocation (indicated by white arrow) of B7-H4 in the presence of LMB. Anti-B7-H4 mAb 3C8, polyclonal antibodies G-18 and H-108 were used. Calnexin was used as a cytoplasmic marker (PI (red, DNA) and cy5 (blue, B7-H4)). (**b**) 20 μg total protein from each fraction (C or N) was blotted with anti-B7-H4 3C8, anti-α-tubulin or anti-PARP. (Anti-α-tubulin and anti-PARP were used for testing the house keeping protein or nuclear protein, respectively, for confirming equivalent loading). (**c**) B7-H4 nuclear translocation (white arrows indicate nuclear B7-H4) was detected in MDA-MB-453, MCF-7, THP-1 and U937 cells by confocal immunofluorescence microscopy. Cells were treated with solvent alone (−) or 10 ng/ml LMB (+) for 24 h and immunostained using anti-B7-H4 3C8. (PI (red,DNA) and cy5 (blue, B7-H4)).

tumor progression through negatively regulating T-cells proliferation, while nuclear B7-H4 has no obvious effect on negative regulation of T-cell function.

In the present study, we have identified B7-H4 as a cytoplasmic-nuclear shuttling protein. Several lines of evidence support our finding. First, the coding sequences of B7-H4 contain a putative NLS motif (246 KRRSH 250). Second, LMB treatment caused translocation of B7-H4 from the cytoplasm to the nucleus in HEK293 and in cancer cell lines SK-BR-3, MDA-MB-453, MCF-7, U937 and THP-1, implying a cytoplasmic-nuclear shuttling for B7-H4. Third, a point mutation in the NLS of B7-H4 abolished the LMB-induced nuclear localization. Finally, cell fractionation showed that LMB induced a significant shift of B7-H4 from the cytoplasmic fraction into the nuclear fraction. So far, there have been very few studies on the nuclear localization of B7 family members. A recent study demonstrated the presence of nuclear expression of B7-H1, another B7 family member. The nuclear upregulation of B7-H1 was induced by doxorubicin and involved in PI3K/AKT pathway.[16] It will be interesting to test whether PI3K/AKT pathway affects the nuclear localization of B7-H4. In fact several dual localization proteins have been reported previously.[17] For example, many growth factors or growth factor receptors belong to dual localization protein, such as fibroblast growth factor-3 (FGF-3),[18] insulin-like growth factor-1[19] and so on. Our study gives an enlightenment that B7-H4 is a dual localization protein and it might act not only as a membrane protein.

It is well documented that surface B7-H4 is responsible to its negative regulatory function of T-cell immunity via the inhibition of T-cell activation, proliferation and cytokine production. In ovarian cancer, tumor-associated macrophages express surface B7-H4 and suppressed tumor-associated antigen-specific T-cell immunity.[7] The present study showed that the membrane B7-H4 was inversely correlated with the density of TILs, supporting the role of surface expression of B7-H4 in the inhibition of T-cell responses. The soluble B7-H4 protein from stably transfected cells, suppressed the proliferation and cytokine production of purified T cells. The point mutation of NLS motif resulted in the production of more soluble and active form of B7-H4. Collectively, compelling evidence indicates that the surface B7-H4 is mainly responsible for its negative regulatory function of T-cell immunity, which may contribute to immune evasion by tumors.

We have noted that there is controversy regarding the function of soluble B7-H4. Azuma *et al.*[20] and Kamimura *et al.*[21] showed that soluble B7-H4 might enhance T-cell-mediated autoimmune responses. However, Simon *et al.*[8] and Thompson *et al.*[22] reported that soluble B7-H4 might be a tumor biomarker for ovarian cancer and renal cell cancer, respectively, which suggests that soluble B7-H4 acts as a T-cell-negative regulatory molecule to dampen

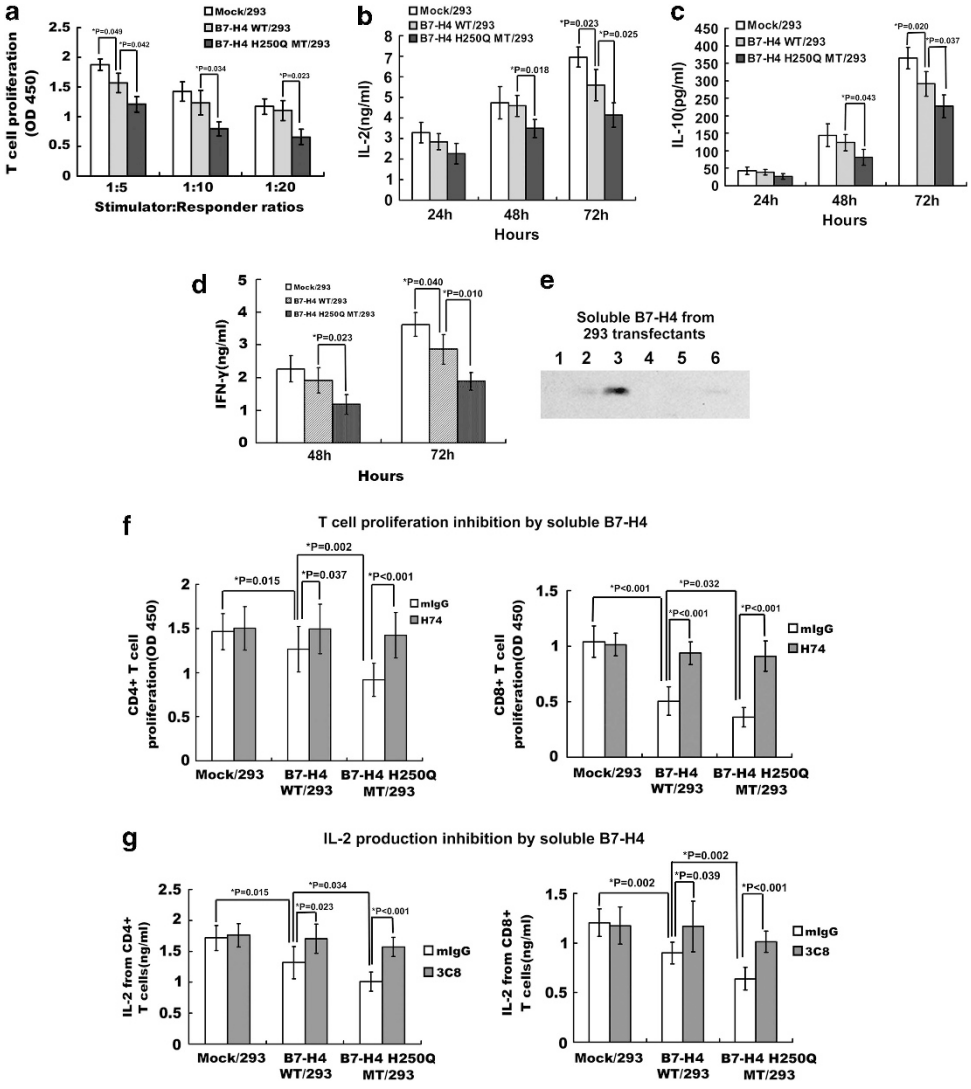

Figure 4. The effects of wild-type B7-H4 and NLS mutant on negative regulation of T-cell activation. Purified T cells from human were stimulated with plate-bound anti-CD3 (0.5 μg/ml) and 293 transfectants expressing GFP or B7-H4-GFP or B7-H4 H250Q-GFP. (**a**) The proliferation of T cells was measured after 72 h by CCK8 assay. Aliquots of supernatant were collected at the indicated time, IL-2 (**b**), IL-10 (**c**) and interferon-γ (**d**) were detected by Enzyme-linked immunosorbent assay (ELISA). Error bars indicate s.d. of triplicate measurements. These data are representative of three independent experiments. (**e**) Mock/293, B7-H4 WT/293 and B7-H4 H250Q MT/293 cells were seeded at 2×10^5 cells/ml into flasks, respectively, in the absence or presence of matrix metalloproteinase inhibitor (minnesota multiphasic personality inventory, MMPI) for 24 h. Cells were collected and counted. Supernatants from same number of 293 transfectants were collected and concentrated tenfold by Millipore Amicon Ultra-15. The levels of soluble B7-H4 released into the supernatants were determined by western blotting. 1-Mock/293; 2-B7-H4 WT/293; 3-B7-H4 H250Q MT/293; 4-Mock/293 + MMPI; 5- B7-H4 WT/293 + MMPI; 6-B7-H4 H250Q MT/293 + MMPI. (**f**) The assay of soluble B7-H4 inhibition on T-cell proliferation was carried as described in method. T cells were stimulated by plate-bound anti-CD3. Proliferation of T cells was measured after 72 h by CCK8 assay. Error bars indicate s.d. of triplicate measurements. (**g**) IL-2 production inhibition by soluble B7-H4 was measured by ELISA as described in method. Error bars indicate SD of triplicate measurements. These data are representative of three independent experiments.

host immunity and contributes to tumor immune evasion. Zang *et al.*[3] collected soluble B7x-Ig (that is, B7-H4-Ig) from supernatants and detected the T-cell inhibitory effect using an experimental system like ours. Thus, the function of soluble B7-H4 need to be further explored. It is possible that soluble B7-H4 from different sources may have distinct structure and function. Kamimura *et al.*[21] thought that soluble B7-H4 might bind different receptors under various conditions, as some B7 family members regulate T-cell activation positively and negatively via distinct receptors. Azuma *et al.*[20] proposed another possibility that soluble B7-H4 might be made from an alternative spliced form leading to different functions. Therefore, the functional significance of soluble B7-H4 remains unclear and requires further detailed investigation.

Very little is known about the effect of intracellular B7-H4 on tumorigenesis. Cheng *et al.*[23] transfected a B7-H4-GFP expression construct into B7-H4-negative human ovarian cancer cell line, SKOV3. The B7-H4-GFP fusion protein was found in the cytoplasm of transfected cells. They further showed that B7-H4 promoted cell proliferation, cell adhesion, migration and invasion. SKOV3 cells expressing B7-H4 gained growth advantage in the xenograft model.[23] Salceda *et al.*[24] reported that endogenous B7-H4 protected cells from apoptosis. They found that overexpression of B7-H4 in a human ovarian cancer cell line increased tumor

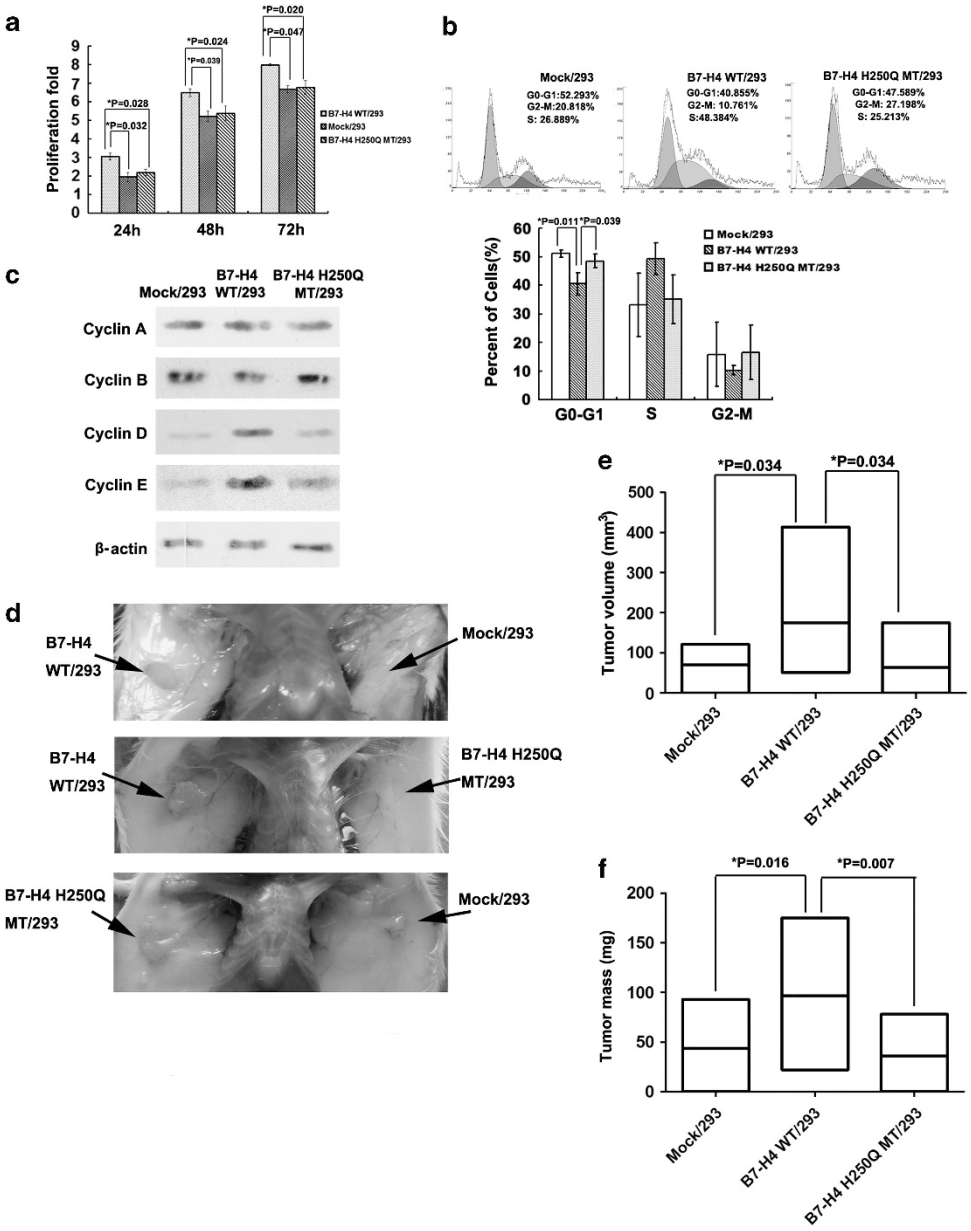

Figure 5. B7-H4 promotes the growth of HEK293 cells *in vitro* and accelerates G1/S phase progression in HEK293 cells. (**a**) Growth curves of mock/293, B7-H4 WT/293 and B7-H4 H250Q MT/293 cells measured by CCK8. Equal numbers of each cell type were incubated in medium containing 5% fetal calf serum. At 24, 48 and 72 h, CCK8 were added and OD 450 was detected. Data represents the fold difference in OD 450 compared with that at 0 h. Results are mean ± s.e.m. from two separate experiments. (**b**) The fluorescence-activated cell sorting (FACS) analysis indicated that B7-H4 WT promoted G1/S phase transition, while B7-H4 H250Q MT did not. (**c**) B7-H4 WT could upregulated the expression of Cyclin D1 and Cyclin E in 293 transfectants. (β-Actin was used for testing the house keeping protein for confirming equivalent loading). (**d**) Mock/293, B7-H4 WT/293 and B7-H4 H250Q MT/293 cells were mixed with Matrigel and subcutaneously injected into contralateral side of the mice as described in method. Aspect of the tumors *in vivo* and before dissection in the representative mice of three groups were photographed. (**e**) 24 Mice were divided into three group (8 mice per group). Cells were injected into right flank. After 8 weeks mice were killed and tumors were dissociated. Tumor volumes on 8th week were evaluated as described in method. (**f**) Tumor weight on 8th week was measured.Data was analyzed by SPSS program.

Figure 6. The effect of nuclear B7-H4 on RCC cell lines. (**a**) The surface and intracellular expression of B7-H4 in RCC cell lines 786-O, Caki-1 and ACHN detected by flowcytometry. (**b**) Caki-1 and ACHN were transfected with plasmids expressing B7-H4 WT, B7-H4 H250Q MT or vector alone. 24 h after transfection, GFP + cells were selected by flowcytometry and 3C8 staining showed GFP + cells successfully expressed B7-H4 WT or B7-H4 H250Q MT. (**c**) Growth curves of Mock/Caki-1, B7-H4 WT/Caki-1 and B7-H4 H250Q MT/Caki-1 cells measured by CCK8. Equal numbers of each cell type were incubated in medium containing 5% FCS. At 24, 48 and 72 h, CCK8 were added and OD 450 was detected. Data represents the fold difference in OD 450 compared with that at 0 h. Results are mean ± s.e.m. from two separate experiments. (**d**) Mock/Caki-1, B7-H4 WT/Caki-1 and B7-H4 H250Q MT/Caki-1 cells were treated with various concentration of docetaxel or doxorubicin. Cell viability was assayed by CCK8. $^{*}P<0.01$, B7-H4 WT/Caki-1 compared with Mock/Caki-1; $^{\#}P<0.01$, B7-H4 WT/Caki-1 compared with B7-H4 H250Q MT/Caki-1. (**e**) Mock/ACHN, B7-H4 WT/ACHN and B7-H4 H250Q MT/ACHN cells were treated with various concentration of docetaxel or doxorubicin. Cell viability was assayed by CCK8. $^{*}P<0.01$, B7-H4 WT/ACHN compared with Mock/ACHN; $^{\#}P<0.01$, B7-H4 WT/ACHN compared with B7-H4 H250Q MT/ACHN.

formation in severe combined immunodeficiency mice, and protected the epithelial cells from anoikis. Knockdown of B7-H4 mRNA and protein expression by small intefering RNA in breast cancer cell line increased caspase activity and apoptosis. Similarly Chen *et al.*[25] showed that intracellular B7-H4 could suppress bile duct epithelial cell apoptosis. In this study, we observed that

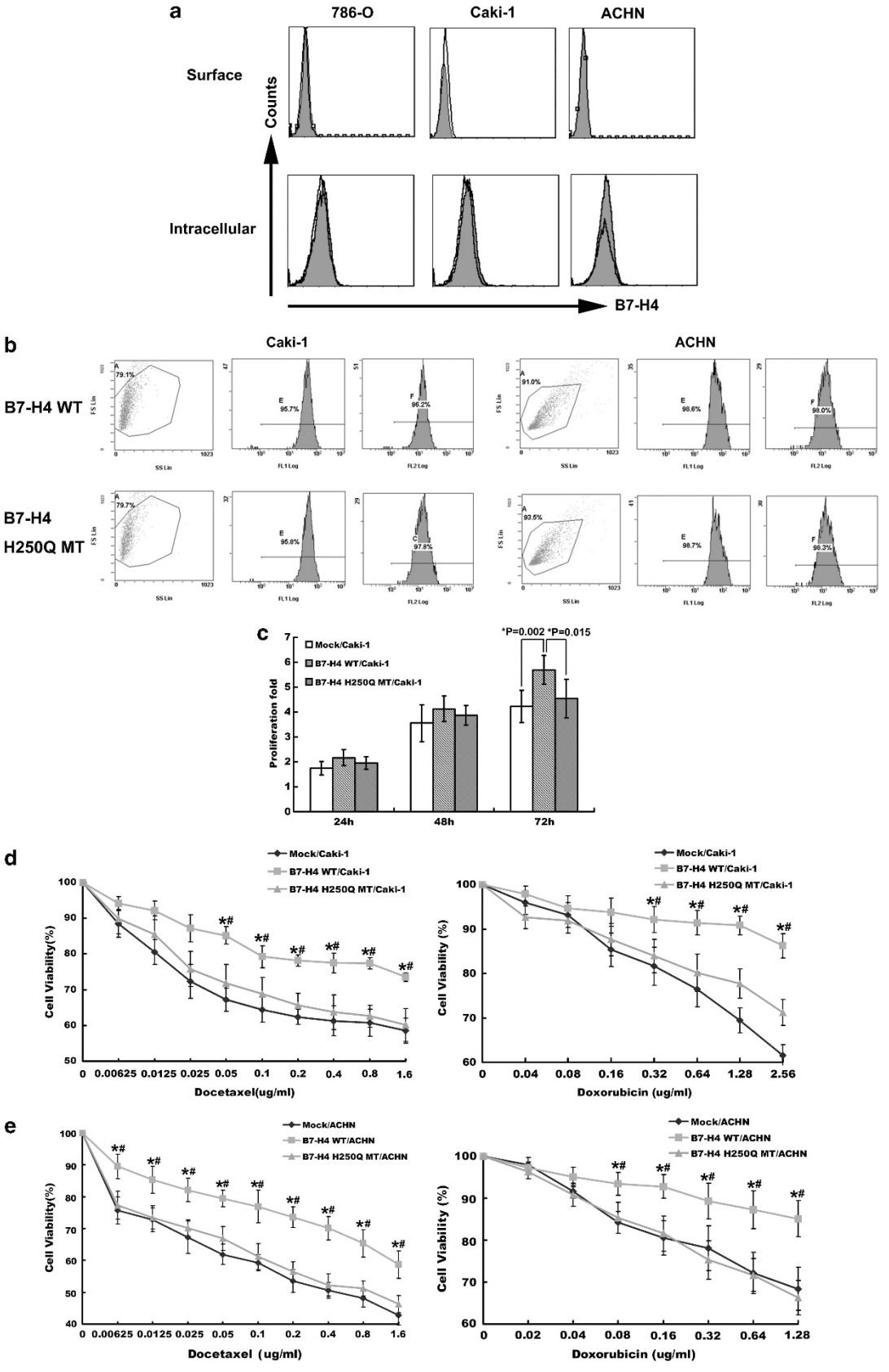

mutation of the NLS motif have a profound impact on B7-H4-mediate cell proliferation and cell cycle progression. The B7-H4 stably transfected HEK293 cells, exhibited a higher proliferation rate *in vitro*, and has the ability to promote G1/S phase transition. A point mutation of B7-H4 NLS motif abolished the effect of B7-H4 on cell proliferation and cell cycle. The results from xenograft mice model showed that B7-H4 WT/293 cells demonstrated stronger tumorigenicity than Mock/293 and B7-H4 H250Q MT/293 cells, suggesting that B7-H4 could promote cancer development not only through immune evasion pathway, but also through regulating tumor tumorigenecity. Additionally, in contrast to the membrane B7-H4, the nuclear B7-H4 was not associated with the density of TILs. Taken together, our results revealed that nuclear B7-H4 seems to have a crucial role in cell proliferation and cell cycle progression. Besides the effect on cell cycle regulation, it is reported that endogenous B7-H4 could effectively protect cells from apoptosis through decreasing caspase activity.[25] In our research we found that B7-H4 WT could effectively protect cells from apoptosis induced by docetaxel and doxorubicin, while B7-H4 H250Q MT could not. So we speculated that nuclear B7-H4 might regulate the expression of genes involved in cell apoptosis. In future research we will investigate how nuclear B7-H4 regulates cell apoptosis.

It is known that chemoresistance is a typical feature of RCC. Conventional treatment of RCC consists of immunotherapy using recombinant human interleukin-2 (rhIL-2) and interferon-α.[26] Up to now some factors have been identified in the development of drug resistance. For example, increased P-glycoprotein expression might be an important cause of clinical chemoresistance.[27] Vasko *et al.*[28] identified 15 proteins involved in the cisplatin resistance in RCC cell lines. In this study, we demonstrated that overexpression of B7-H4 in RCC cells further enhanced resistant to chemodrugs even though these cells are genereally resistant to chemotherapy. Concerning the high expression rate in clinical RCC specimen, we speculated that B7-H4 might be one of the factors involved in the drug resistance of RCC.

It is known that AKT and ERK pathways have critical roles in cell survival, proliferation and tumor growth.[29,30] Recently Wang *et al.*[31] has demonstrated that B7-H4 regulated cell proliferation through inhibiting Erk, Jun, P38 and AKT pathways in activated cells. However, up to now there is no report about whether these pathways are involved in the effect of subcellular localization of B7-H4 on cell proliferation. Some previous reports showed that AKT could protect cells from apoptosis through regulating the nuclear-cytoplasmic traffick of some molecules. For example, Parsa *et al.* and Crane *et al.*[32,33] have shown a direct relationship between AKT activation pathway and B7-H1 expression. They demonstrated that B7-H1 is a downstream target of AKT.[32,33] Ghebeh *et al.*[16] have shown that PI3K/AKT pathway is involved in the nuclear translocation of B7-H1. Huang *et al.*[34] indicated that nuclear translocation of epidermal growth factor receptor is dependent on phosphorylation at Ser229 by AKT. Kurebayashi *et al.*[35] found that PI3K/AKT pathway controls nulear localization of ROR_{Υ} in the Th17 cells differentiation. It is interesting to investigate whether AKT pathway plays a role in the nuclear translocation and cell proliferation-promoting function of B7-H4.

In summary, our result revealed that B7-H4 could express on the membrane, in the cytosol and/or the nucleus in RCC tissues. The membrane and nuclear localization of B7-H4 correlate with poor prognosis in RCC. We further showed that B7-H4 could shuttle between the cytoplasm and nucleus. The direct effect of B7-H4 on proliferation and cell cycle was associated with its nuclear localization. This study provides new insights into the role of B7-H4 in proliferation and cell cycle. Future studies on intracellular B7-H4 function may lead to the development of novel therapeutic approaches against tumors.

MATERIALS AND METHODS

Cell culture and antibodies

The cell lines SK-BR-3, MDA-MB-453, MCF-7, HEK293, THP-1 and U937 were purchased from the cell bank of Chinese Academy of Sciences. Cell lines were cultured according to the instruction of the cell bank of Chinese Academy of Sciences. The anti-B7-H4 mAb (clone 3C8) was produced by our laboratory.[10] Other antibodies were purchased from commercial sources: anti-B7-H4 mAb (clone H74), anti-PARP mAb and anti-α-tubulin mAb (eBioscience, San Diego, CA, USA), anti-calnexin mAb (Millipore, Billerica, MA, USA), anti-B7-H4 polyclonal antibodies (clone G-18 and H-108) (Santa Cruz Biotechnology, Santa Cruz, CA, USA), anti-CD3 and anti-CD8 mAb (R&D systems, Minneapolis, MN, USA), anti-Cyclin D mAb (Invitrogen, Carlsbad, CA, USA), anti-Cyclin E mAb (Invitrogen, USA), anti-Cyclin A mAb (Santa Cruz, USA), anti-Cyclin B mAb (Cell Signaling, Beverly, MA, USA).

RCC tissue

A total of 82 specimens were collected from patients undergoing radical nephrectomy in the Department of Urology, the second affiliated hospital of Soochow University. The final staging, grading and histological diagnosis were based on the pathology report. Ethics approval was obtained from the local Institutional Review Board (IRB) committee.

Immunohistochemical staining

The B7-H4 protein was detected by immunoperoxidase staining method. Slides with fixed paraffin-embedded sections were deparaffinized in serial grades of xylene followed by rehydration in sequentially increasing dilutions of ethanol. Antigen retrieval was then performed using microwave heating in 10 mM sodium citrate buffer (pH *6.0) for 8 min. Endogenous peroxidase activity was blocked with 3.0% hydrogen peroxide for 15 min. The sections were incubated with the anti-B7-H4 mAb clone 3C8 (1 μg/ml) at room temperature for 1 h,and then washed three times in phosphate-buffered saline (PBS) followed by incubation with biotinylated secondary antibody (1:200) at room temperature for 1 h. After three washes in PBS, the avidin-biotin-horseradish peroxidase complex (1:100) was applied and incubated at room temperature for 1 h in a humid chamber followed by three washes in PBS. The sections were counter-stained with Mayer's hematoxylin and mounted in aqueous mountant.

The sections were scored as positive if the tumor cells showed positive staining in the membrane, cytosol, and/or nucleus. All the slides were evaluated and graded independently in a blinded fashion by two investigators. Signal intensity and percentage signal coverage of each region were scored according to the Allred scoring system.[36] The signal intensity was graded from 0–3 (0, none; 1, weak; 2, intermediate; 3, strong), and the percentage of positive tumor cells was scored on a scale from 1–5 (1, <1; 2, 1–10; 3, 10–30; 4, 30–60; 5, >60%). For example, if a specimen was not stained by the antibodies, it will be scored as $0+1$(Allred score-1, that is, negative).

Evaluation of TILs in RCC tissues

TILs in tumor nest were determined according to immunostaining for CD4 and CD8. Five areas in tumor nest with the most intense TILs were selected at low magnification ($\times 40$), and then TILs were counted and recorded at high power field ($\times 200$ magnification). Results from the five areas were averaged and used in the statistical analysis. The sections with less than 60 TILs per high power field were defined as low infiltration group, and the sections with more than 60 TILs per high power field were defined as high infiltration group. The cut-off value of 60 TILs per high power field for low/high infiltrating assessment in tumor nest was set at the median value of all the sections.

LMB treatments

For immunofluorescence staining, cells were seeded in 6-well plate and cultured for 24 h. Cells were then treated with 10 ng/ml LMB (Sigma-Aldrich, St Louis, MO, USA) or solvent alone (0.1% methanol) for 24 h.

For the fractionation experiments, SK-BR-3 cells and the stably transfected cells were seeded into ten culture flasks and grown to 80% confluence. LMB was added to five flasks to obtain final concentration of 5 ng/ml, while control flasks received solvent alone (0.1% methanol). Cells were then cultured for an additional 24 h.

Immunofluorescence staining

The cultured cells were washed for 10 min with PBS, fixed with 4% paraformaldehyde in PBS for 15 min, washed for a further 10 min with PBS, permeabilized with 0.5% Triton x-100 in PBS for 15 min, washed in PBS twice for 10 min each. Cells were blocked with 1% bovine serum albumin (BSA) in PBS for 0.5 h and immunostained with primary antibodies (1:100 dilution in PBS with BSA) for 1 h at 37 °C. For SK-BR-3 cells the primary antibodies used were anti-B7-H4 mAb clones 3C8 and polyclonal antibodies H-108, G-18, and for other types of cells only 3C8 was used. Cells were further washed three times with PBS for 10 min each and subsequently stained for 1 h with secondary cy5-conjugated antibody (1:1000 dilution in PBS with BSA) or for 15 min with PI at room temperature. Cells were mounted onto glass slides using FluorSave (Merck) and imaged at 22 °C using an inverted FluoView confocal microscope (Leica TCS SP2 CLSM) coupled with $\times$20/0.70NA objective lens. Images were acquired and analyzed using the Leica TCS SP-2 software.

Nuclear and cytoplasmic fractionation

LMB-treated cells and control cells were washed twice with PBS, and dispersed by 0.2% EDTA. Then cells were collected. The cytoplasmic and nuclear fractions were prepared using the Nuclear and Cytoplasmic Protein Extraction Kit purchased from Beyotime Institute Biotechnology (Nantong, China) according to the instruction. The fractionation efficiency was assessed by antibodies against α-tubulin and PARP.

Western blotting

Proteins were separated by 12% SDS–polyacrylamide gel electrophoresis, and gels were equilibrated for 30 min in transfer buffer (20% methanol, 190 mM glycine, 25 mM Tris). Proteins were blotted onto polyvinylidene difluoride membranes (Millipore), which were then blocked for 1 h in 5% BSA/PBS at room temperature, washed with PBS containing 0.1% Tween-20 (PBST), and immunostained for 1 h at room temperature with the primary antibody in 5% BSA/PBS. The following primary antibodies were used: anti-B7-H4 mAb 3C8, anti-PARP mAb (1:10 000) and anti-α-tubulin mAb (1:1000), anti-Cyclin A mAb (1:500), anti-Cyclin B mAb (1:1000), anti-Cyclin D mAb (1:500), anti-Cyclin E (1:500). Blots were then washed and labeled for 1 h with goat anti-mouse Ig F(ab′)$_2$-HRP conjugate (1:1000 in 5% BSA/PBST; Millipore). After washing extensively in PBST, blots were immersed in ECL detection reagent (Cell Signaling) and exposed to X-Omat AR film (Eastman Kodak Co., Rochester, NY, USA).

Construction of transfected cell lines

Human B7-H4 cDNA was amplified by real time–PCR and cloned into the pIRES2-EGFP expression vector. The NLS mutant of B7-H4 was made by site-directed mutagenesis. This mutant contains a single point mutation, H250Q, in the putative NLS of B7-H4. The plasmid harboring the mutated gene was designated as pIRES2-EGFP-B7-H4-H250Q. All constructions were confirmed by DNA sequencing.

HEK293 cells were transfected with the expression plasmids pIRES2-EGFP-B7-H4 and pIRES2-EGFP-B7-H4-H250Q and vector alone. Selection of stable clones were initiated in G418 (0.5 mg/ml) containing medium 48 h after transfection. Transfectants were cultured in parallel in selection selected based on high expression of B7-H4 every 2–3 weeks by fluorescence-activated cell sorting (FACS). The resulting stably transfected cell lines were designated as Mock/293 (GFP+), B7-H4 WT/293 (GFP+/B7-H4+) and B7-H7 H250Q MT/293 (GFP+/B7-H4+).

In vitro analysis of T-cell proliferation

Peripheral blood mononuclear cells were isolated from healthy donors by Ficoll-Biocoll Separation Solution as described previously.[37] Human T cells were enriched by magnetic cell sorting using the Easysep human T-cell enrichment kit (catalog no. 19051). For T-cell proliferation assays, 96-well flat bottom microtiter plates were coated with 0.5 μg/ml anti-CD3 mAb at 4 °C overnight. Wells were washed extensively and plated with purified T cells at 1×10^6 cells/ml. Three stably transfected HEK293 cell lines (mock/293, B7-H4 WT/293 and B7-H4 H250Q MT/293) were grown and harvested. Cells were then pretreated with mitomycin and added to the wells at the indicated effector: target (E/T) ratios: 1:5, 1:10 and 1:20. The cell proliferation was measured at 72and 96 h after incubation using the cell counting kit-8 (CCK8) assay. The proliferation assays were performed in triplicate.

For the soluble B7-H4 inhibition assay, human CD4+ and CD8+ T cells were purified by using magnetic beads (Miltenyi Biotec, Auburn, CA, USA). 96-well flat bottom microtiter plates were coated with 100 μl anti-CD3 mAb (0.5 μg/ml) at 4 °C overnight and then the wells were washed with PBS for three times, and coated with 200 μl supernatant from same density of stably transfected cells for 2 h at 37 °C. Wells were washed three times with PBS and plated with 100 μl RPMI 1640 medium containing 2 μg mIgG or anti-B7-H4 mAb (3C8). After 15 min, 100 μl purified human CD4+ and CD8+ T cells (1×10^6/ml) were added into the wells and incubated with mIgG or anti-B7-H4 mAb for 72 h. T-cells proliferation was measured by CCK8 assay and IL-2 production was assayed by enzyme-linked immunosorbent assay .

Cytokine enzyme-linked immunosorbent assay

Aliquots of supernatant were collected at 48 h after initiation of cell cultures. IL-2, IL-10 and interferon-γ were measured by enzyme-linked immunosorbent assay using mAbs and recombinant cytokine standards from R&D Systems.

Cell proliferation assay

Cell proliferation was quantitated by CCK8 assay to generate a growth curve over 5 days. Mock/293, B7-H4 WT/293 and B7-H4 H250Q MT/293 cells were seeded at 2×10^4 cells per well in a 96-well plate (day 0) and incubated for a further 3 days. On each successive day, cell number per well was determined by CCK8 assay. Statistical differences between cell types on each day were determined by analysis of variance (ANOVA).

Tumor xenograft experiments

Mock/293, B7-H4 WT/293 and B7-H4 H250Q MT/293 cells (2×10^7) in 100 μl PBS with matrigel were inoculated into the 4-week old male severe combined immunodeficiency mice (Slac Laboratory Animal, Shanghai, China). To compare the tumor formation in one mouse, 12 mice were divided into three groups and in each group every mouse was inoculated with Mock/293 cells on the left side and B7-H4 WT/293 cells on the right side, or with B7-H4 H250Q MT/293 cells on the left side and B7-H4 WT/293 cells on the right side, or with Mock/293 cells on the left side and B7-H4 H250Q MT/293 cells on the right side. Furthermore, 24 mice were divided into three groups randomly, and each group was implanted with one of the three transfectants, Mock/293, B7-H4 WT/293 or B7-H4 H250Q MT/293. Cells were injected on the right side. Tumor formation was monitored by palpation and caliper measurement. The formed tumors were dissociated and tumor volume was calculated using the formula $v = ab^2/2$, where a is the longest perpendicular dimension and b is the shortest dimension of the tumor. All animal experiments were performed in complete compliance with institutional guidelines for animal care.

Measurement of cytotoxicity

Caki-1 and ACHN transfectants (5×10^3 per well) were seeded in 96-well plates. After 6 h, cells were treated with indicated concentration of doxorubicin or docetaxel, respectively. In parallel, 5×10^3 cells per well were seeded in 96-well plates and treated with PBS. The viability of cells was determined by CCK8 assay.

Statistical analyses

SPSS version 13.0 (SPSS, Chicago, IL, USA) was used for statistical analyses. P-values < 0.05 were considered significant.

CONFLICT OF INTEREST

The authors declare no conflict of interest.

ACKNOWLEDGEMENTS

We are grateful to Yu-ming Hu for his assistant in animal experiment; Wei Sun for collecting the clinical specimens; Ying Chen for her help in immunohistochemical analysis; and Kehua Yu as well as Yu Shen for their technical assistance in flow cytometry. This work was supported by National Nature Science Foundation of China (Grant No. 30901361); Natural Science Fund for Colleges and Universities in Jiangsu Province (Grant No. 09KJB310013); National Program on Key Basic Research Project (973 Program, Grant No. 2013CB530501); Program for Changjiang Scholars and Innovative Research Team (Grant No. IRT0849); National Natural Science Foundation

of China (Grants No. 30930085); A Project Funded by the Priority Academic Program Development of Jiangsu Higher Education Institutions (PAPD); Jiangsu Planned Projects for Postdoctoral Research Funds (No. 0702053); National University Student Innovation of Soochow University.

REFERENCES

1 Flies DB, Chen L. The new B7s: playing a pivotal role in tumor immunity. *J Immunother* 2007; **30**: 251–260.
2 Sica GL, Choi IH, Zhu G, Tamada K, Wang SD, Tamura H *et al.* B7-H4, a molecule of the B7 family, negatively regulates T cell immunity. *Immunity* 2003; **18**: 849–861.
3 Zang X, Loke P, Kim J, Murphy K, Waitz R, Allison JP. B7x: a widely expressed B7 family member that inhibits T cell activation. *Proc Natl Acad Sci USA* 2003; **100**: 10388–10392.
4 Prasad DV, Richards S, Mai XM, Dong C. B7S1, a novel B7 family member that negatively regulates T cell activation. *Immunity* 2003; **18**: 863–873.
5 Tringler B, Zhuo S, Pilkington G, Torkko KC, Singh M, Lucia MS *et al.* B7-H4 is highly expressed in ductal and lobular breast cancer. *Clin Cancer Res* 2005; **11**: 1842–1848.
6 Krambeck AE, Thompson RH, Dong H, Lohse CM, Park ES, Kuntz SM *et al.* B7-H4 expression in renal cell carcinoma and tumor vasculature: associations with cancer progression and survival. *Proc Natl Acad Sci USA* 2006; **103**: 10391–10396.
7 Kryczek I, Zou L, Rodriguez P, Zhu G, Wei S, Mottram P *et al.* B7-H4 expression identifies a novel suppressive macrophage population in human ovarian carcinoma. *J Exp Med* 2006; **203**: 871–881.
8 Simon I, Zhuo S, Corral L, Diamandis EP, Sarno MJ, Wolfert RL *et al.* B7-H4 is a novel membrane-bound protein and a candidate serum and tissue biomarker for ovarian cancer. *Cancer Res* 2006; **66**: 1570–1575.
9 Tringler B, Liu W, Corral L, Torkko KC, Enomoto T, Davidson S *et al.* B7-H4 overexpression in ovarian tumors. *Gynecol Oncol* 2006; **100**: 44–52.
10 Chen LJ, Sun J, Wu HY, Zhou SM, Tan Y, Tan M *et al.* B7-H4 expression associates with cancer progression and predicts patient's survival in human esophageal squamous cell carcinoma. *Cancer Immunol Immunother* 2011; **60**: 1047–1055.
11 Arigami T, Uenosono Y, Ishigami S, Hagihara T, Haraguchi N, Natsugoe S. Clinical significance of the B7-H4 coregulatory molecule as a novel prognostic marker in gastric cancer. *World J Surg* 2011; **35**: 2051–2057.
12 Jiang J, Zhu Y, Wu C, Shen Y, Wei W, Chen L *et al.* Tumor expression of B7-H4 predicts poor survival of patients suffering from gastric cancer. *Cancer Immunol Immunother* 2010; **59**: 1707–1714.
13 Awadallah NS, Shroyer KR, Langer DA, Torkko KC, Chen YK, Bentz JS *et al.* Detection of B7-H4 and p53 in pancreatic cancer: potential role as a cytological diagnostic adjunct. *Pancreas* 2008; **36**: 200–206.
14 Quandt D, Fiedler E, Boettcher D, Marsch WC, Seliger B. B7-H4 expression in human melanoma: its association with patients' survival and antitumor immune response. *Clin Cancer Res* 2011; **17**: 3100–3111.
15 Miyatake T, Tringler B, Liu W, Liu SH, Papkoff J, Enomoto T *et al.* B7-H4 (DD-O110) is overexpressed in high risk uterine endometrioid adenocarcinomas and inversely correlated with tumor T-cell infiltration. *Gynecol Oncol* 2001; **106**: 119–127.
16 Ghebeh H, Lehe C, Barhoush E, Al-Romaih K, Tulbah A, Al-Alwan M *et al.* Doxorubicin downregulates cell surface B7-H1 expression and upregulates its nuclear expression in breast cancer cells: role of B7-H1 as an anti-apoptotic molecule. *Breast Cancer Res* 2010; **12**: R48.
17 Arnoys EJ, Wang JL. Dual localization: proteins in extracellular and intracellular compartments. *Acta histochem* 2007; **109**: 89–110.
18 Kiefer P, Acland P, Pappin D, Peters G, Dickson C. Competition between nuclear localization and secretory signals determines the subcellular fate of a single CUG-initiated form of FGF3. *EMBO J* 1994; **13**: 4126–4136.
19 Tan DSW, Cook A, Chew SL. Nucleolar localization of an isoform of the IGF-1 precursor. *BMC Cell Biol* 2002; **3**: 17.
20 Azuma T, Zhu G, Xu H, Rietz AC, Drake CG, Matteson EL *et al.* Potential role of decoy B7-H4 in the pathogenesis of rheumatoid arthritis: a mouse model informed by clinical data. *PloS Med* 2009; **6**: e1000166.
21 Kmimura Y, Kobori H, Piao J, Hashiguchi M, Matsumoto K, Hirose S *et al.* Possible involvement of soluble B7-H4 in T cell-mediated inflammatory immune responses. *Biochem Biophys Res Commun* 2009; **389**: 349–353.
22 Thompson RH, Zang X, Lohse CM, Leibovich BC, Slovin SF, Reuter VE *et al.* Serum-soluble B7x is elevated in renal cell carcinoma patients and is associated with advanced stage. *Cancer Res* 2008; **68**: 6054–6058.
23 Cheng L, Jiang J, Gao R, Wei S, Nan F, Li S *et al.* B7-H4 expression promotes tumorigenesis in ovarian cancer. *Int J Gynecol Cancer* 2009; **19**: 1481–1486.
24 Salceda S, Tang T, Kmet M, Munteanu A, Ghosh M, Macina R *et al.* The immunomodulatory protein B7-H4 is overexpressed in breast and ovarian cancers and promotes epithelial cell transformation. *Exp Cell Res* 2005; **306**: 128–141.
25 Chen Y, Guo G, Guo S, Shimoda S, Shroyer KR, Tang Y *et al.* Intracellular B7-H4 suppresses bile duct epithelial cell apoptosis in human primary biliary cirrhosis. *Inflammation* 2010; **34**: 688–697.
26 Guida M, Colucci G. Immunotherapy for metastatic renal cell carcinoma: is it a therapeutic option yet? Ann Oncol 2007; **18**(Suppl 6): vi149–vi152.
27 Mickisch GH. Chemoresistance of renal cell carcinoma: 1986-1994. *World J Urol* 1994; **12**: 214–223.
28 Vasko R, Mueller GA, von Jaschke AK, Asif AR, Dihazi H. Impact of cisplatin administration on protein expression levels in renal cell carcinoma: a proteomic analysis. *Eur J Pharmacol* 2011; **670**: 50–57.
29 Vivanco I, Sawyers CL. The phosphatidylinositol 3-kinase AKT pathway in human cancer. *Nat Rev Cancer* 2002; **2**: 489–501.
30 Boucher MJ, Morisset J, Vachon PH, Reed JC, Lainé J, Rivard N. MEK/ERK signaling pathway regulates the expression of Bcl-2, Bcl-X(L) and Mcl-1 and promotes survival of human pancreatic cancer cells. *J Cell Biochem* 2000; **19**: 355–369.
31 Wang X, Hao J, Metzger DL, Ao Z, Chen L, Ou D *et al.* B7-H4 treatment of T cells inhibits ERK, JNK,p38, and AKT activation. *PloS One* 2012; **7**: e28232.
32 Crane CA, Panner A, Murray JC, Wilson SP, Xu H, Chen L *et al.* PI(3)kinase is associated with a mechanism of immunoresistance in breast and prostate cancer. *Oncogene* 2009; **28**: 306–312.
33 Parsa AT, Waldron JS, Panner A, Crane CA, Parney IF, Barry JJ *et al.* Loss of tumor suppressor PTEN function increases B7-H1 expression and immunoresistance in glioma. *Nat Med* 2007; **13**: 84–88.
34 Huang WC, Chen YJ, Li LY, Wei YL, Hsu SC, Tsai SL *et al.* Nuclear translocation of EGFR by AKT-dependent phosphorylation enhances BCRP/ABCG3 expression in gefitinib-resistant cells. *J Biol Chem* 2011; **286**: 20558–20568.
35 Kurebayashi Y, Nagai S, Lkejiri A, Ohtani M, Lchiyama K, Baba Y *et al.* PI3K-Akt-mTORC1-S6K1/2 axis controls Th17 differentiation by regulating Gfi1 expression and nuclear translocation of ROR_{Υ}. *Cell Rep* 2012; **1**: 360–373.
36 Allred DC, Clark GM, Elledge R, Fuqua SA, Brown RW, Chamness GC *et al.* Association of p53 protein expression with tumor cell proliferation rate and clinical outcome in node-negative breast cancer. *J Natl Cancer Inst* 1993; **85**: 200–206.
37 Fei F, Yu Y, Schmitt A, Rojewski MT, Chen B, Greiner J *et al.* Dasatinib exerts an immunosuppressive effect on CD8+ T cells specific for viral and leukemia antigens. *Exp Hematol* 2008; **36**: 1297–1308.

Supplementary Information accompanies the paper on the Oncogene website (http://www.nature.com/onc)